

NUMERICAL ASSESSMENT TECHNIQUE ON DAMAGES OF RIVER FLOOD AND INUNDATIONS CAUSED BY LARGE FLOODS

TATSUFUMI MIYAZAKI⁽¹⁾ & SHOJI FUKUOKA⁽²⁾

⁽¹⁾ Graduate School of Science and Engineering, Chuo University, Kasuga 1-13-27, Bunkyo-ku, Tokyo 112-8551, JAPAN,
E-mail: miyazaki@civil.chuo-u.ac.jp

⁽²⁾ Research and Development Initiative, Chuo University, Kasuga 1-13-27, Bunkyo-ku, Tokyo 112-8551, JAPAN,
E-mail: sfuku@tamacc.chuo-u.ac.jp

ABSTRACT

Successive large floods exceeding the designed discharge occurred in the Kagetsu River in July 3 and 14, 2012. The floods caused serious damages such as levee breaches and flood inundations in densely residential area. In this paper, we analyzed both flood behavior in the river channel and inundation area by numerical analyses of quasi-three dimensional flows and two-dimensional bed variations. Causes of levee breaches were investigated by field survey and numerical computation results of velocity distributions and bed variations during the floods. Numerical simulation showed that the river-crossing structure (Yuuta Bridge) caused severe overbank flows by the driftwood accumulations and large inundation over dense housing areas.

Keywords: driftwoods, flood flow, levee breach, inundation, numerical computation

1. INTRODUCTION

The Kagetsu River lying on the northwest of Oita Prefecture in Japan (see Figure 1) joins the upper Chikugo River. The drainage area of the Kagetsu River is about 136.1 km². Figure 2 shows the planform of ministerial management section of the Kagetsu River. In this area, the river channel runs through built-up areas with mean slope of 1/250 and width of 60m. The Arita River having the comparable drainage area meets the Kagetsu River at a right angle at 5.3km point (see Figure 2). The main problem of the Kagetsu River is the discharge capacity of the river channel.

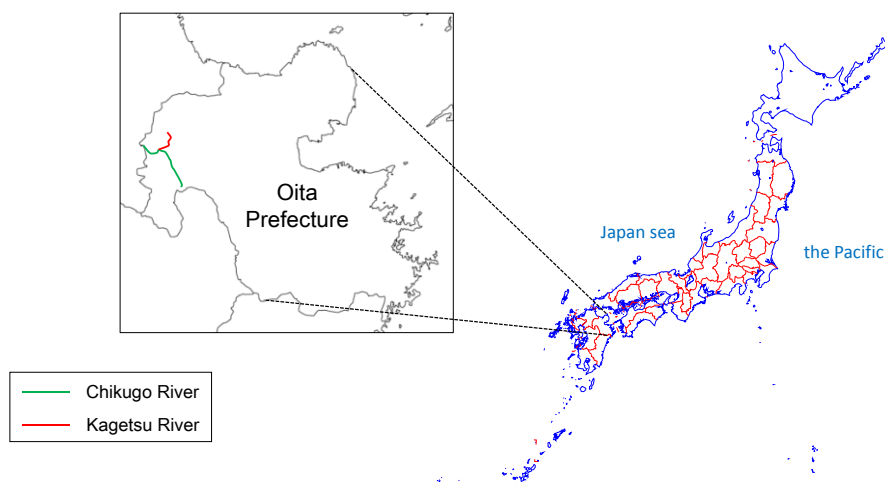


Figure 1. Location of the Kagetsu River.

Successive large floods exceeding the designed discharge (1,200m³/s) occurred in the Kagetsu River at July 3 and July 14, 2012. The peak discharge of these floods were about 1,284m³/s and 1,349m³/s, respectively. Levee breaches occurred at the right bank of 6.0km and the left bank of 5.8km points (see Figure 3), and overbank flows occurred at concrete embankment in the downstream area of the Arita River confluence during the first flood. It brought large inundations of approximately 121 hectares and 721 buildings were damaged by the inundation water as shown in Figure 2. Emergency rehabilitation was conducted place after the July 3 flood and levee breaches were escaped during the July 14 flood, but overbank flows inundated approximately 79 hectares areas and 282 buildings were damaged. It is believed that water level increase due to the driftwood accumulations around the Yuuta Bridge at 4.7km point (see Figure 3) expanded the flood inundation damages at the middle Kagetsu River (see Figure 2). The driftwood accumulations around a bridge during flood events have been serious problem for many middle and small-scale rivers in Japan. Fujimori et al. (2008) quantitatively estimated fluid forces acting on the bridge railing from hydraulic experiments. Maeno et al. (2014)

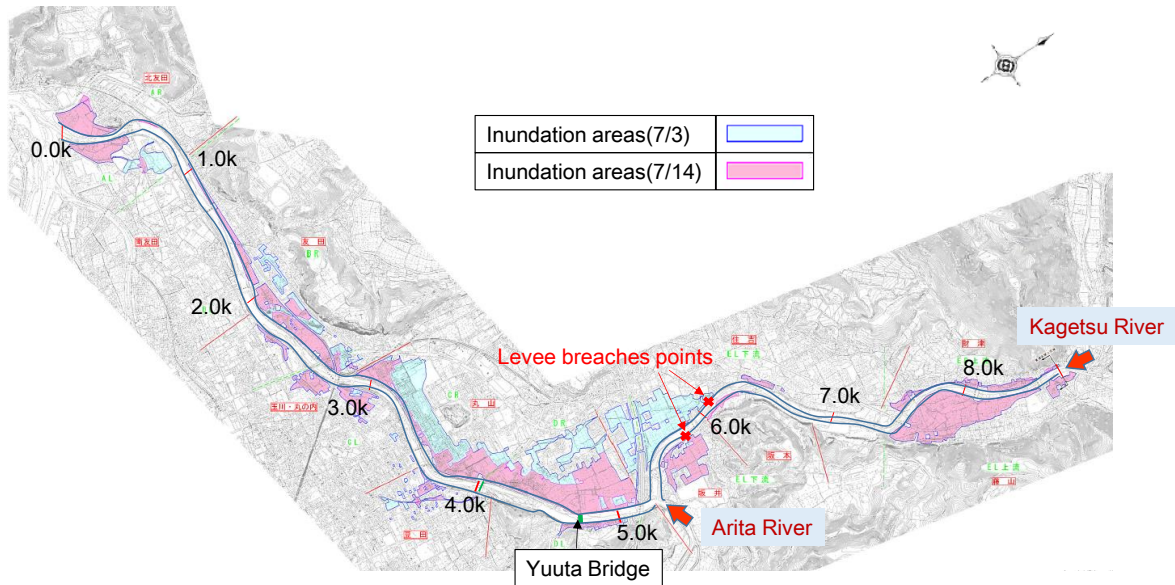


Figure 2. Inundation areas of the Kagetsu River basin at July 2012.

clarified that the force acting on the bridge could be estimated by using the three-dimensional flow model. But three dimensional models have extremely high computational cost. Moreover there are few studies about resistances and blockage effects of the bridge covered by driftwoods because it is difficult to observe the amount over time of the driftwood accumulations around a bridge during floods.

In this study, we constructed the numerical model which could compute flood flows and bed variations in the river channel and inundation flows in the built-up area considering the driftwood accumulations around the Yuuta Bridge based on the depth-integral model. By using the numerical model and measured data during the Kagetsu River floods, we investigated the cause of the levee breaches, and mechanics of the overbank flows and return flows over the concrete embankment from the inundation area to the river channel.



(a) Right bank of 6.0km point.



(b) Left bank of 5.8km point.

Figure 3. Soil levee breaches of the Kagetsu River during the first flood.



(a) Driftwood accumulations around the Yuuta Bridge.



(b) Overbank flows around the Yuuta Bridge.

Figure 4. Driftwood accumulations and overbank flows around the Yuuta Bridge.

2. ANALYSIS METHOD AND CONDITIONS

2.1 Analysis method

In this paper, we developed the calculation method to solve simultaneously flood flows and bed variations in the river channel and inundation flows in the built-up area considering the driftwood accumulation around the Yuuta Bridge. The BVC method by Uchida and Fukuoka (2011) was adopted in order to analyze flood flows in the channel. And unsteady two-dimensional flow analysis was adopted for the inundation flow analysis.

The BVC method is composed of a set of governing equations of Eq. [1] to Eq. [5] for the following unknown quantities: water depth h , Depth Averaged (DA) horizontal velocities U_i , DA horizontal vorticities Ω_i , water surface velocities u_{si} and bottom velocities u_{bi} . The bottom velocity is derived by integrating horizontal vorticities respect to depth (Eq. [1]).

$$u_{bi} = u_{si} - \Omega_j h \quad [1]$$

where, u_{bi} is bottom velocity in i direction, u_{sj} is water surface velocity, h is water depth and Ω_j is DA horizontal vorticity.

Bottom velocity by Eq. [1] is obtained by depth-integrated horizontal vorticity equation [2] and water surface velocity equation [3] in addition to shallow water equations [4], [5]. In this study, Eq. [2] to Eq. [5] are converted to the general curvilinear coordinate system.

$$\frac{\partial \Omega_i h}{\partial t} = ER_{\sigma i} + P_{\omega i} + \frac{\partial h D_{\omega ij}}{\partial x_j} \quad [2]$$

where, $ER_{\sigma i}$ is rotation term of vertical vorticity, $P_{\omega i}$ is production term of vorticity from the bottom thin vortex layer and $D_{\omega ij}$ is horizontal vorticity flux due to convection, rotation, dispersion and turbulence diffusion.

$$\frac{\partial u_{si}}{\partial t} + u_{sj} \frac{\partial u_{si}}{\partial x_j} = -g \frac{\partial z_s}{\partial x_i} + P_{si} \quad [3]$$

where, g is the acceleration of gravity, z_s is water level and P_{si} is production term due to shear stress acting on thin water surface layer.

$$\frac{\partial fh}{\partial t} + \frac{\partial f U_j h}{\partial x_j} = 0 \quad [4]$$

$$\frac{\partial U_i}{\partial t} + U_j \frac{\partial U_i}{\partial x_j} = -g \frac{\partial z_s}{\partial x_i} - \frac{1}{\rho h \Delta x \Delta y} (D_i + P_i) + \frac{\partial T_{ij}}{\rho h \partial x_j} - \frac{\tau_{bi}}{\rho h} \quad [5]$$

where, T_{ij} is horizontal shear stress due to turbulence and vertical velocity distribution, ρ is water density, τ_{bi} is bed shear stress, D_i is drag force of bridge piers, P_i is force on a bridge railing and f is occupancy ratio of water considering bridge railing and piers. Detail discussions of drag forces of bridge piers D_i , force on a bridge railing P_i and occupancy ratio of water f were given in section 2.2. The two dimensional bed-variation analysis took into account the bed load. A rate of the bed load transport was calculated by Ashida and Michiue formula (Ashida & Michiue., 1972).

2.2 Analysis conditions

The discharge hydrograph at 8.6km point of the Kagetsu River and inflow discharge hydrograph from the Arita River used for the upstream boundary conditions were given by the runoff analysis. The downstream boundary condition was given by the water level hydrograph estimated at 0.0km point which was created with considering the shape of the measured

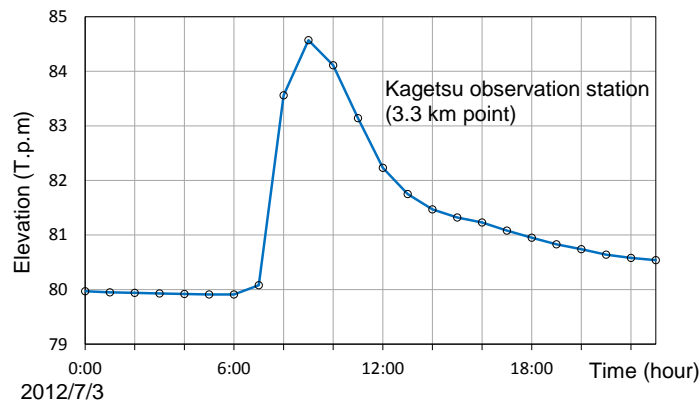


Figure 5. Observed water level hydrographs.

water level hydrograph at the Kagetsu observation station at 3.3 km point (see Figure 5) and the flood mark elevations at 0.0km point. The Manning roughness coefficients were determined so as to explain the longitudinal distribution of flood marks obtained after each flood. They were set as 0.035 and 0.025 in the channel and inundation areas, respectively. Bed elevations in the river channel were given by the cross-sectional profiles of the Kagetsu River measured at 200 m intervals in August 2010. Particle size distributions used for the bed variation analysis shown by Figure 6 were determined from the data of bed materials survey of the study area in 2010.

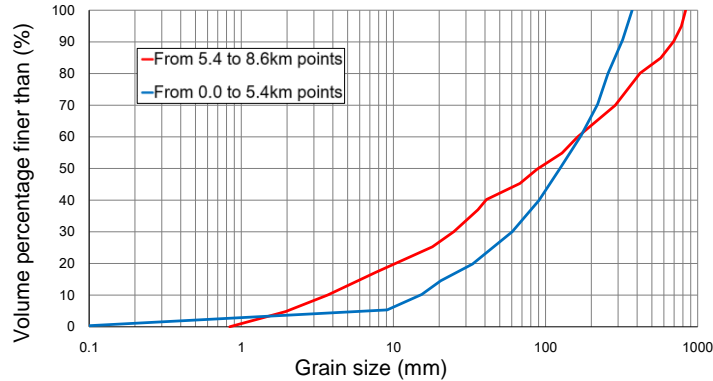
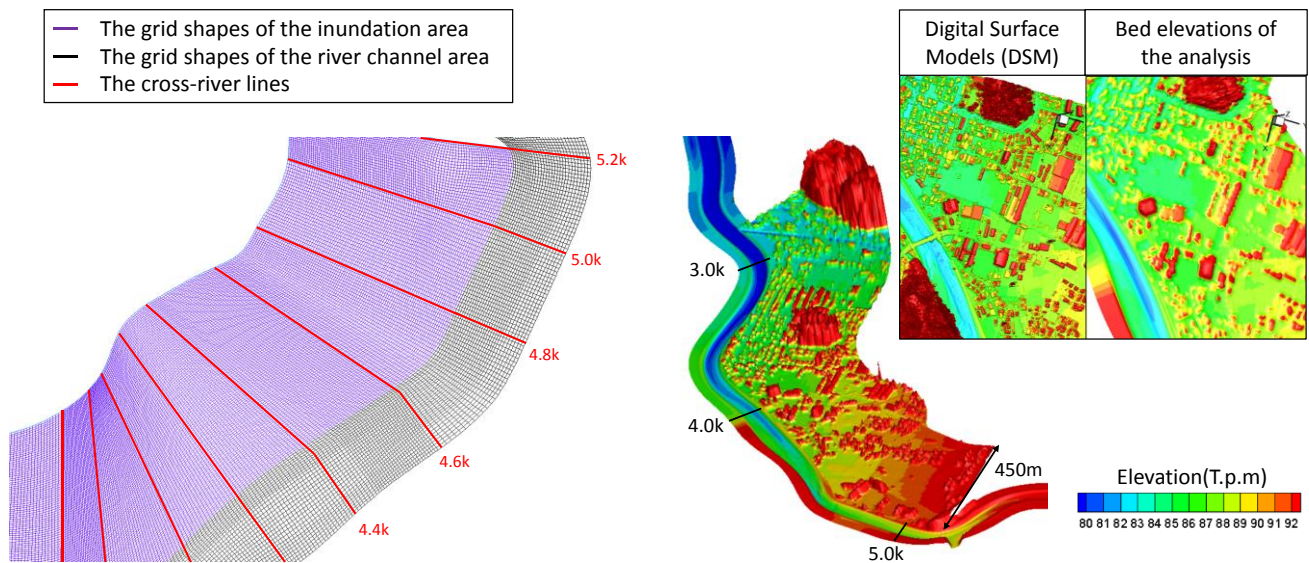


Figure 6. Particle size distributions used to the analysis.

2.3 Method for evaluating the height and location of buildings in the inundation areas and the cross-river structure

2.3.1 Method for evaluating the height and location of buildings in inundation areas

The height and location of buildings and the road network patterns of inundation areas are extremely important for an inundation simulation at a built-up area. Bed elevations of inundation areas are usually given by the Digital Elevation Models (DEM) which represents the elevations of the ground surface measured by the aerial laser profiling (e.g., P.D. Bates et al. (2000)) and the effects of the buildings on inundation flows are evaluated by the equivalent roughness coefficient and occupancy ratio of water of each computational grid. But, because many buildings exist in the built-up area around the Kagetsu River, it is difficult to set properly the equivalent roughness and occupancy ratio of water for each computational grid. Akiyama et al. (2007) made the computational grids along the buildings and road networks and directly considered the height of the buildings existing at the built-up areas by using the Digital Surface Models (DSM) which represent the elevation of the ground surface and aboveground features measured by the aerial laser profiling. But it takes enormous effort and time to make the computational grids in built-up area along the buildings and road networks. For this reason, we created the computational grids in the built-up area by simply expanding the computational grids made for the river channel by using the general curvilinear coordinate to the inundation area as shown in Figure 7 (a). In order to consider the location of the buildings adequately, the computational grids were made finely and the bed elevations of built-up area were given by using the DSM. Figure 7(b) shows the DSM data and the bed elevations of the numerical model at the middle Kagetsu River. The bed elevations of the numerical model could reproduce the height and location of buildings and road network patterns very well.



(a) The grid shapes around the built-up area that is adapted for the numerical analysis.

(b) DSM data and the bed elevations of the numerical analysis.

Figure 7. The grid shapes and surface bed elevations around the built-up area.

2.3.2 Method for evaluating the cross-river structure

In the Kagetsu River floods, it was expected that driftwood accumulations around the Yuuta Bridge railing and piers obstructing flood flows and the considerable water level increase induced severe overbank flows at the just upstream of the Yuuta Bridge. For this reason, it was needed to consider the resistances and blockage effects of the Yuuta bridge railing and piers in the numerical analysis.

In this study, Eq. [4] and Eq. [5] were solved for the general curvilinear coordinate system at the computational grids including the Yuuta bridge railing and piers. They were derived by considering the volume ratio of the Yuuta bridge railing and piers and their resistance. Because the plan form of the river channel around the Yuuta Bridge is almost straight and the bridge was constructed at almost a right angle to the river channel, it can be assumed that the flow resistance of the bridge railing and piers mainly work in the main stream direction. So, the drag force received from the Yuuta bridge piers in the main stream direction was given as

$$D_i = \frac{1}{2} \rho C_D U_i U A_1 \quad [6]$$

where, U is depth averaged horizontal velocity, C_D is drag coefficient, A_1 is projected area of river bridge piers in main stream direction. Because the amount over time of the driftwood accumulations around the Yuuta Bridge piers during the flood events are unapparent, the drag coefficient was set as the value generally used for a river bridge pier ($C_D=1.0$) and the projected area considered only for the Yuuta Bridge piers. On the other hand, it was apparent from the photographs that the driftwood accumulations on the Yuuta Bridge railing heavily obstructed flowing of the floods. In order to consider the driftwood accumulations, we assumed the impermeable wall above the Yuuta Bridge railing and made the flood water unable to flow over the wall as shown in Figure 8. The force received from the Yuuta Bridge railing in the main stream direction was given by the form of the drag force as shown by Eq. [7].

$$P_i = \frac{1}{2} \rho C_D u_{si} u_s A_2 \quad [7]$$

where, u_s is water surface velocity, A_2 is projected area of the Yuuta Bridge railing in main flow direction. Drag coefficient of the Yuuta Bridge railing was determined so as to explain the longitudinal distribution of the flood marks observed after each flood. The occupancy ratio of water f found in Eq. [4] was determined so that the flood flow was unable to flow over the Yuuta Bridge railing at the computational grids including the Yuuta Bridge railing and piers as shown in Figure 8.

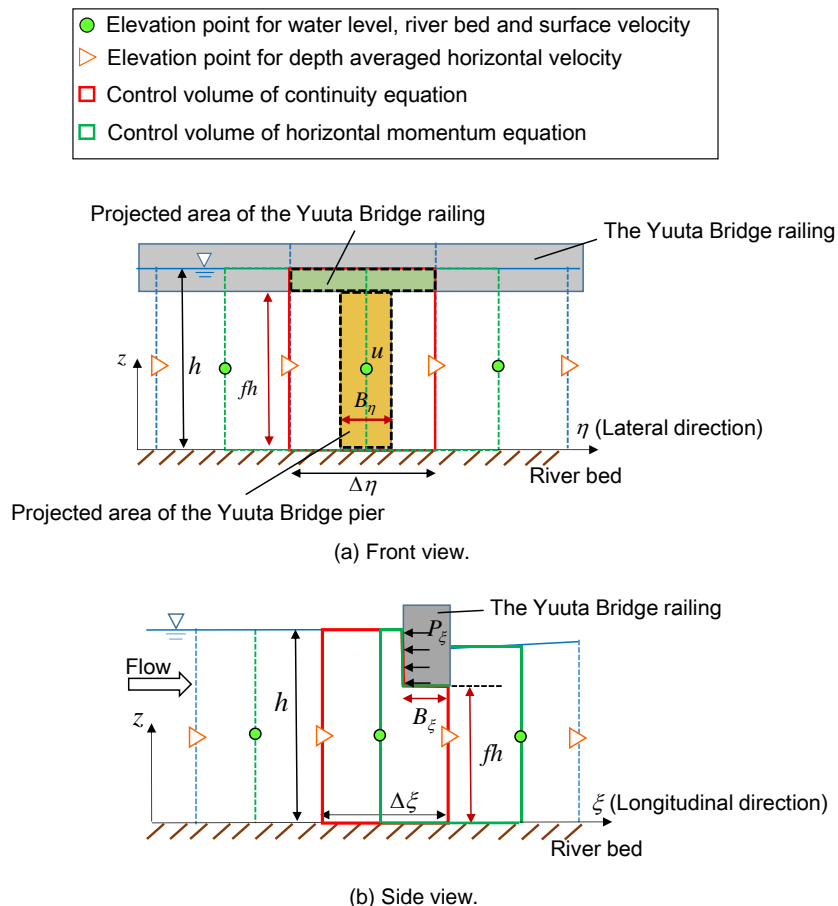
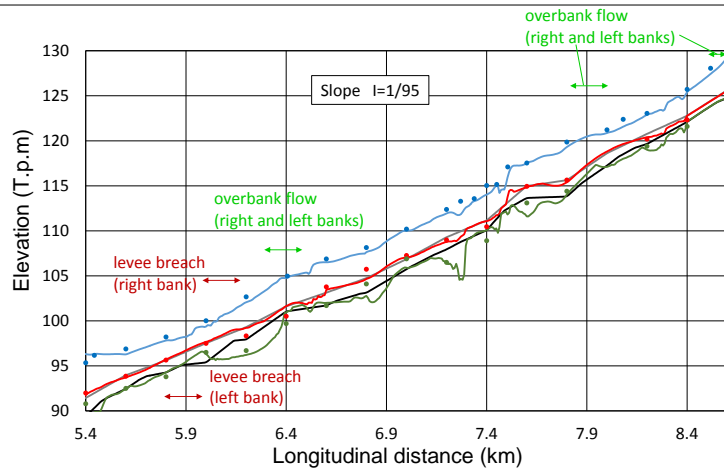
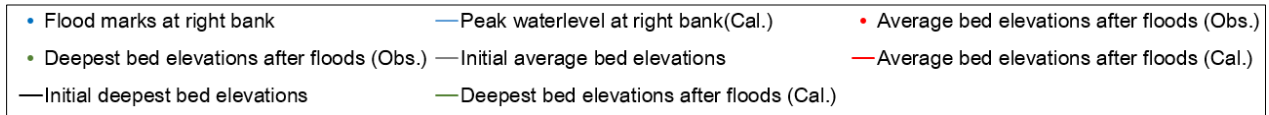


Figure 8. Computation method considering the driftwood accumulation around the Yuuta bridge railing.

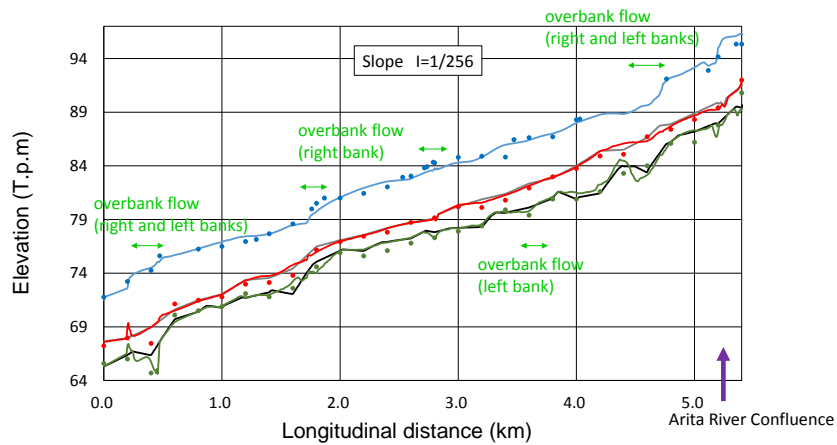
3. NUMERICAL ANALYSIS RESULTS

3.1 Comparison between numerical analysis results and observed data

Figure 9(a) and (b) show the longitudinal distributions of the computed peak-water level and flood marks in the first flood and the longitudinal distributions of the bed elevations before and after the flood. The computed peak-water levels could explain the longitudinal distribution of the flood marks. But the computed peak-water levels were lower than the flood



(a) Upstream reach.



(b) Downstream reach.

Figure 9. Comparison between the longitudinal distributions of computed peak-water level and the flood marks in the first flood and longitudinal distributions of the bed elevations before and after the floods.

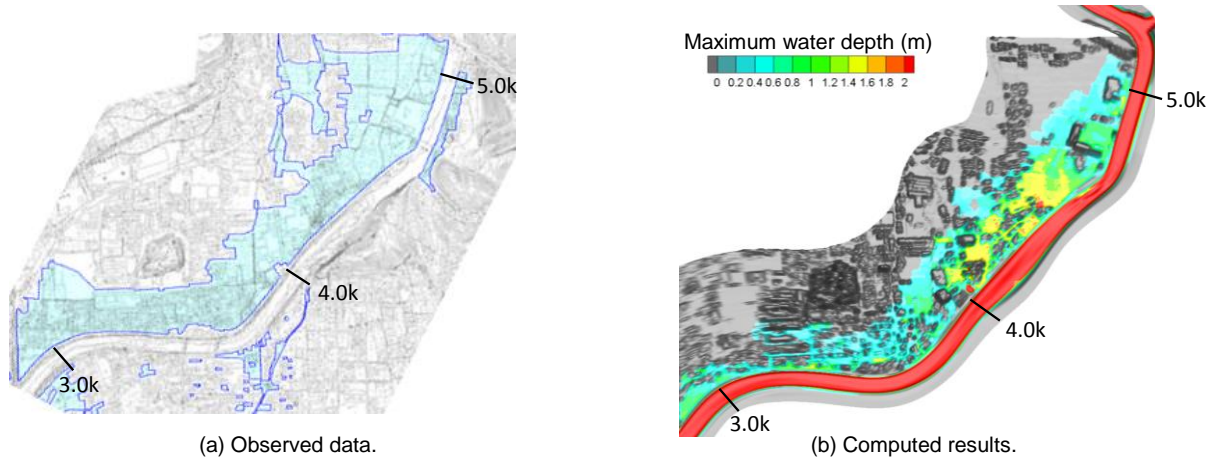


Figure 10. Comparison between observed and computed inundation areas and maximum water depth distributions in the first flood.

marks in some locations. In addition, the computed bed elevations after the floods almost agreed with the observed average and lowest bed-elevations. Figure 10(a) and (b) show the observed inundation areas after the first flood and the computed inundation areas and maximum water depth distributions at the first flood. The computed inundation area of the first flood could almost reproduce the observed data. The relatively poor reproducibility around the 3.0km point (see Figure 10(a), (b)) was due to the absent of considering the inundation water from the tributary flowing into the Kagetsu River around 2.8km point.

3.2 Flow and bed variation around the levee breach points

Figure 11 shows the contour map of the bed variations and depth averaged velocity vectors at the peak of the first flood from 5.8 km to 6.8 km points at the Kagetsu River. Higher velocities concentrated to the outer bank side due to the river planform, and they caused the bed scouring at the right bank in 6.0km point and at the left bank in 5.8km point where the levee breaches occurred as shown in Figure 11.

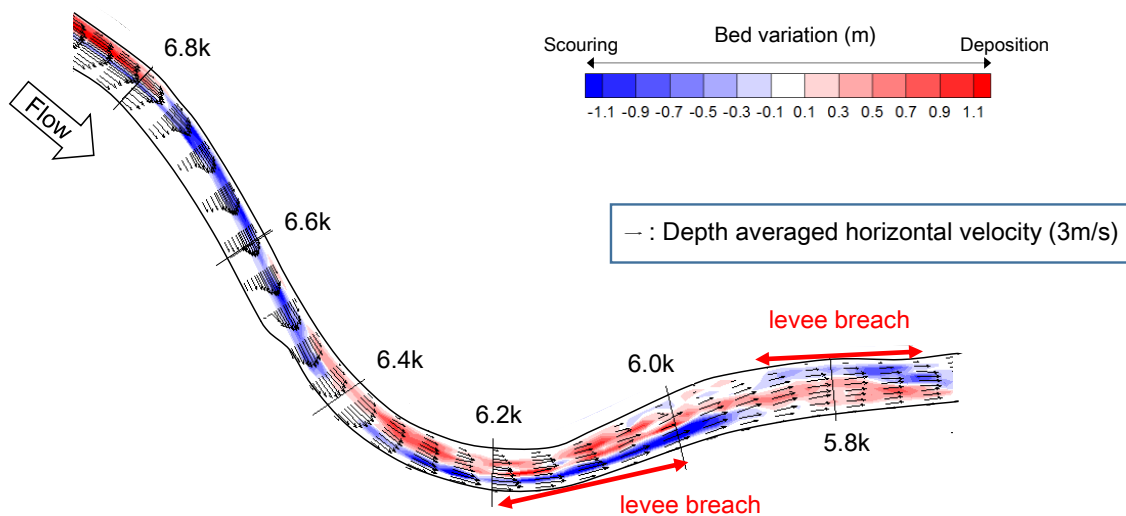


Figure 11. Contour map of computed bed variations and velocity vectors around the levee breaches area at the peak of the first flood.

Figure 12(a) and (b) show cross-sectional distributions of the computed depth-averaged velocity, river bed levels before and after the floods and peak water levels at 6.0km and 5.8km points. The computed maximum velocity was 6.9 m/s and the bed scouring was at least 1.0m near the right bank at 6.0km point (see Figure 12(a)). Similarly, the high velocity and bed scouring occurred near the left bank of 5.8km point. In addition, the computed maximum water level was lower than the levee height as shown in Figure 12(a) and (b). It is suggested that the bed scouring was the most influential factor for the levee breaches at the first flood in the Kagetsu River.

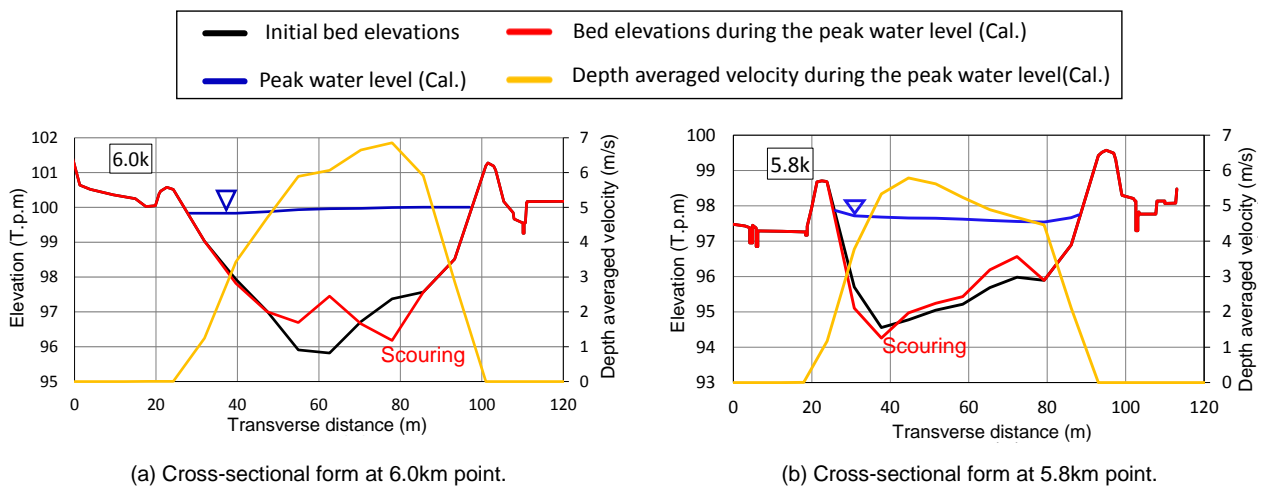


Figure 12. Computed bed variations and velocity distributions at the peak of the first flood at 6.0km and 5.8km points.

3.3 Inundation in the built-up area around the middle Kagetsu River

Figure 13 (a) and (b) show the contour maps of inundation water depth computed at the beginning of the overbank flows and at the flood peak during the first flood, respectively. The computed water level at the Yuuta Bridge already reached the elevation of the bridge railing at 8:40am July 3. In this time, overbank flows didn't occur yet. But overbank flows



Figure 15. Photograph of return flows of inundation water to the river around 4.0km point at 9:40am July 3.

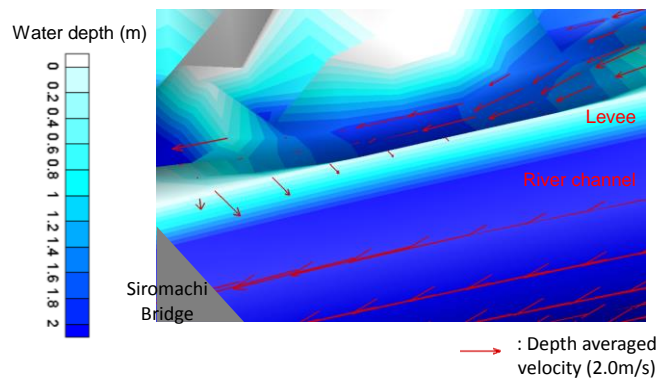


Figure 16. Contour map of computed water depth and depth-averaged velocity of channel flow and inundation flow around 4.0km point at 9:30am July 3.

4. CONCLUSIONS

The following conclusions were drawn by using the numerical model and data measured during the Kagetsu River floods.

- 1) We developed the numerical model which could explain flood flows and bed variations in the Kagetsu River and inundation flows in the built-up area by considering driftwood accumulations at the Yuuta Bridge. Here, the height and location of buildings and road network patterns at the built-up area were directly given by the Digital Surface Models (DSM) to examine the behavior of the inundation water in the built-up area.
- 2) It is suggested that bed scouring was the most influential factor for breaches of soil levees at the first flood in 2012 in the Kagetsu River.
- 3) Inundation water passing through the built-up area returned into the river channel over concrete embankment around the Siromachi Bridge, since the densely-packed buildings blocked further spreading of the inundation water and the bed elevation around the Siromachi Bridge were higher than surrounding areas.
- 4) Because the ground slope in the built-up area was almost similar to the slope of the river channel, houses in the built-up area received large fluid force and heavy damages from the inundation water during the floods.

REFERENCES

- Fujimori Y., Ochi Y., Hayama S., Shiraishi H., and Watanabe M. (2008). A driftwood hazard and its countermeasures in steep small-scale river. *Proc. JSCE*, 52, 679–684.
- Maeno S., Yoshida K., and Tanaka R. (2014). Evaluation of hydrodynamic forces acting on bridge under flood in steep medium and small scale rivers. *Proc. JSCE*, 70, 883–888.
- Uchida T., and Fukuoka S. (2011). Numerical simulation of bed variation in a channel with a series of submerged groins. *Proceedings of the 34th IAHR World Congress*, 4292–4299.
- Ashida, K. and Michiue, M. (1972). Study on hydraulic resistance and bed-load transport rate in alluvial streams. *Proc. JSCE*, 206, 59–69.
- P.D. Bates., and A.P.J De Roo. (2000). A simple raster-based model for flood inundation simulation. *Journal of Hydrology* 236, 54-77.
- Akiyama J., Shigeeda M., and Tanabe T. (2009). Numerical simulation of inundation flow with sewer networks in the Onga River basin. *Proc. JSCE*, 53, 829–834.